INTRAMOLECULAR TRIPLET-TRIPLET ENERGY TRANSFER IN SHORT FLEXIBLE BICHROMOPHORIC AMINO ACIDS, DIPEPTIDES AND CARBOXYLIC ACID DIESTER

Miroslav ZABADAL[a1,+], Dominik HEGER[a2], Petr KLÁN[a3,*] and Zdeněk KŘÍŽ[b]

[a] *Department of Organic Chemistry, Faculty of Science, Masaryk University, Kotlářská 2, CZ-611 37 Brno, Czech Republic; e-mail:* [1] *mzabadal@chemi.muni.cz,* [2] *hegerd@chemi.muni.cz,* [3] *klan@sci.muni.cz*

[b] *National Centre for Biomolecular Research, Masaryk University, Kotlářská 2, CZ-611 37 Brno, Czech Republic; e-mail: zdenek@chemi.muni.cz*

Received December 9, 2003
Accepted February 10, 2004

Dedicated to Professor Milan Kratochvíl on the occasion of his 80th birthday.

Efficiencies of the intramolecular triplet-triplet energy transfer (ITET) in various bichromophoric amino acids (glycine, valine, phenylalanine, and sarcosine), dipeptides (glycylglycine, phenylalanylphenylalanine), and a simple diester, with the benzoyl and naphthyl terminal groups serving as donor and acceptor, respectively, have been determined by the steady-state photokinetic measurements. The magnitude of the transfer rate constants ($>10^8$ s^{-1}) and the number of bonds separating the chromophores (8 or 11 atoms) suggest a through-space exothermic exchange mechanism in all cases. The influence of interchromophore distance, the character of the connecting chain as well as of side chains, was evaluated. While the most efficient energy transfer was found in a flexible diester and in valine- and sarcosine-based molecules due to the steric effect of the side hydrocarbon groups, the benzyl groups in the phenylalanine and phenylalanylphenylalanine-based bichromophores had a suppressing effect on ITET. Rigidity of the peptide bond in short bichromophoric compounds causes that a large number of favorable geometries preexist already before excitation; thus the intramolecular processes are controlled by ground-state conformational distribution. Replacing this bond by a less rigid ester moiety would allow that certain unfavorable conformations may coil to favorable ones within the excited-state lifetime (a rotation-controlled photochemical model). Some conclusions were supported by a conformational search of the potential energy surface and molecular dynamics simulations.

Keywords: Triplet-triplet energy transfer; Through-space mechanism; Photokinetics; Bichromophore; Amino acids; Esters; Phenacyl.

+ Present address: Chemistry Department, Rutgers University, 73 Warren Street, Newark, NJ 07102, U.S.A.

Intramolecular triplet-triplet energy transfer (ITET) is a basic photophysical process which has been extensively studied since the mechanism was proposed by Dexter[1] and now it is a field of continuing interest[2]. Triplet-triplet energy transfer is allowed by the electron-exchange mechanism[3] and it is now well established that ITET rates are affected by structural and geometric factors; they are highly sensitive to the distance of separation between donor and acceptor chromophores.

Several studies of ITET in bichromophoric compounds with flexible hydrocarbon spacers have been reported[4–6], including computer simulations and modeling[7]. McGimpsey[8] studied intramolecular singlet-singlet and triplet-triplet energy transfer processes in two bichromophoric peptides. Biery at al.[9] measured directly intramolecular chain diffusion of a polypeptide chain by the determination of ITET between chromophores on the nanosecond time scale. Eaton and his co-workers[10] studied the dynamic flexibility of the coil state of a helix-forming peptide by the end-to-end contact rates. The ITET rates were found to decrease with increasing rigidity of the peptide (such as alanylalanine or prolylproline) chain-backbone and the interchromophore distance.

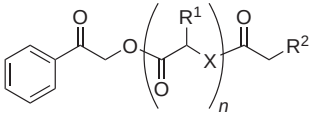

R^2 = phenyl (Ph) or 1-naphthyl (Np)

Compound	R^1	R^2	X	*n*
1aPh	H	Ph	NH	1
1aNp		Np		
1bPh	H	Ph	NH	2
1bNp		Np		
1cPh	$CH(CH_3)_2$	Ph	NH	1
1cNp		Np		
1dPh	CH_2Ph	Ph	NH	1
1dNp		Np		
1ePh	CH_2Ph	Ph	NH	2
1eNp		Np		
1fPh	H	Ph	NCH_3	1
1fNp		Np		
2Ph	H	Ph	O	1
2Np		Np		

Here we present a study of the intramolecular triplet-triplet energy transfer efficiencies in bichromophoric amino acids and dipeptides **1aNp**–**1fNp**, and in diester **2Np** (R^2 = 1-naphthyl), in which benzoyl and naphthyl moieties serve as donor and acceptor chromophores, respectively (the compounds **1aPh**–**1fPh** and **2Ph** (R^2 = phenyl) serve as model compounds). Conventional steady-state kinetic methods were used for calculation of relative ITET rate constants to provide insight into the nature of the interconnecting chains and the data were compared with computer modeling

and simulation results and some other physical analyses. Such an intramolecular through-space process should be fast enough to compete with conformational motion of these (semi)flexible systems since the time required for bimolecular exothermic energy transfer is usually below 100 ps when the chromophores are within the van der Waals radii[11]. Wagner showed that this competition requires a complex kinetic analysis which differs from what is normally employed in ground-state chemistry[12].

EXPERIMENTAL

Melting points were determined on a Kofler hot stage VEB Wagetechnik Rapido 79/2106 and are uncorrected. Infrared spectra were recorded on a FTIR ATI Mattson spectrophotometer in KBr tablets or NaCl cuvettes. NMR spectra were obtained on a Bruker Avance spectrometer 300 (300 MHz for ^{1}H, 75 MHz for ^{13}C). Chemical shifts in ^{1}H NMR spectra are reported in ppm (δ) relative to an internal standard (tetramethylsilane, TMS) at 0.00 ppm, and coupling constants *J* in Hz. Chemical shifts in ^{13}C NMR spectra are reported in ppm (δ) relative to either $CDCl_3$ at 77.23 ppm or DMSO-d_6 at 39.51 ppm. Signal multiplicities in the ^{13}C NMR were determined in APT experiments. NOESY experiments were carried out using a pulse sequence and software provided by the manufacturer. Mass spectra of positive ions obtained by electron impact (EI, 30 eV) were recorded on a GC-MS Fisons Instruments Trio 1000 spectrometer. HPLC measurements were carried out on a LC-20AD (Shimadzu) with an RP-HPLC glass column SGC C-18 or C-8 (7 mm, 3 × 150 mm) where SPD-10A (Shimadzu) was used as UV detector. The UV-VIS spectra and absorption coefficients (ε (acetonitrile) in mol^{-1} dm^3 cm^{-1}) were recorded on a UV 1601 UV-VIS spectrophotometer (Shimadzu) with matched 1.0 cm quartz cells. Acetonitrile was purified by distillation through a vacuum-sealed column (70 cm) packed with glass particles.

Syntheses of Bichromophoric Compounds

Phenacyl bromide was prepared by a standard procedure described elsewhere[13]. *tert*-Butyl bromoacetate was prepared by a procedure described by Newman[14]. Phenacyl esters were prepared according to literature[15]. The synthesis of all bifunctional amino acids and dipeptides **1a**–**1f** and diester **2** was accomplished by a multistep synthesis starting with amino acids **3a**–**3f** or carboxylic acid **6** (Scheme 1). The reaction of phenacyl (2-oxo-2-phenylethyl) bromide and corresponding *N*-(*tert*-butoxycarbonyl) protected amino acids[15] **3a**–**3f** represents the initial step of the syntheses of **1a**–**1f** and the final step in the synthesis of diester **2**. The deprotection of the amino group and the following coupling with a corresponding amino acid or carboxylic acid (phenyl- or 1-naphthylacetic acid) by a conventional DCC-mediated procedure[16] lead to lengthening of the peptide chain or substitution of chain ends with the second chromophore **1a**–**1f**. The synthesis of diester **2** was accomplished by lengthening substituted acetic acid **6** with an acetyl fragment. *tert*-Butyl ester of bromoacetic acid[17] was used for the addition of an acetyl fragment; the following solvolysis provided the corresponding carboxylic acid **8** [18].

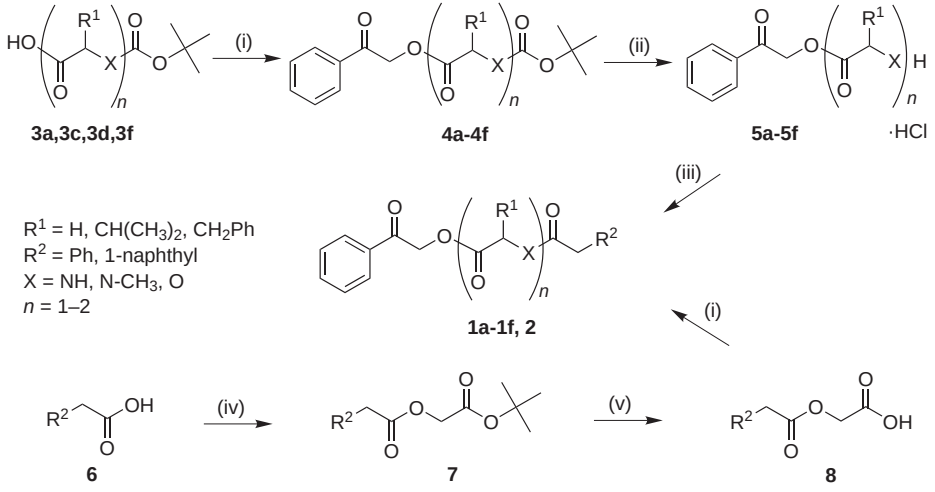

(i) phenacyl bromide, triethylamine/benzene, Ar, r.t., 2 h; (ii) 3 M HCl/AcOEt, ≈0 °C, 1.5-3 h; (iii) (1) *N*,*N*'-dicyclohexylcarbodiimide (DCC), R^2-CH_2-COOH, triethylamine/CH_2Cl_2-DMF, –5 °C, 3 h; (2) r.t., 48 h; (iv) *tert*-butyl bromoacetate, K_2CO_3/acetone, Ar, r.t., 20 h; (v) HCOOH or CF_3COOH ≈0 °C

SCHEME 1

Bichromophoric Compounds

Phenacyl N-(phenylacetyl)glycinate (**1aPh**). White solid, yield 47%, m.p. 120–121 °C (ethanol). For $C_{18}H_{17}NO_4$ (311.3) calculated: 69.44% C, 5.50% H, 4.50% N; found: 70.11% C, 4.48% H, 4.43% N. IR: 3338, 3062, 3032, 2944, 1751 (C=O); 1695 (C=O); 1647 (C=O); 1535, 1428, 1383, 1210, 1190, 728, 695. ^{1}H NMR ($CDCl_3$): 7.89–7.86 m, 2 H, 7.63–7.59 m, 1 H, 7.51–7.46 m, 2 H, 7.35–7.26 m, 5 H (**Ph**$COCH_2$, **Ph**CH_2CO); 5.97 bs, 1 H (NH); 5.37 s, 2 H (PhCOC**H**$_2$); 4.21 d, 2 H, *J*(PhCOCH_2OCOC**H**$_2$,NH) = 5.3 (PhCOCH_2OCOC**H**$_2$); 3.63 s, 2 H (PhC**H**$_2$CO). ^{13}C NMR ($CDCl_3$): 191.6, 171.4, 169.6, 134.6, 134.3, 134.2, 129.7, 129.3, 129.2, 128.0, 127.7, 66.8, 43.7, 41.5. ε_{366} = 2.2.

Phenacyl N-(1-naphthylacetyl)glycinate (**1aNp**). White solid, yield 50%, m.p. 153–154 °C (ethanol/water 4:1). For $C_{22}H_{19}NO_4$ (361.4) calculated: 73.12% C, 5.30% H, 3.88% N; found: 73.63% C, 3.79% H, 3.82% N. IR: 3258, 3069, 2937, 1772 (C=O); 1696 (C=O); 1646 (C=O); 1555, 1404, 1230, 1173, 963, 781, 689. ^{1}H NMR ($CDCl_3$): 7.93–7.90 m, 1 H, 7.80–7.74 m, 4 H, 7.56–7.37 m, 7 H (**Ph**$COCH_2$, **Np**CH_2CO); 5.80 bs, 1 H (NH); 5.23 s, 2 H (PhCOC**H**$_2$); 4.07 d, 2 H, *J*(NpCH_2CONHC**H**$_2$COO,NH) = 5.5 (NpCH_2CONHC**H**$_2$COO); 4.02 s, 2 H (NpC**H**$_2$CO). ^{13}C NMR ($CDCl_3$): 197.5, 172.9, 160.6, 134.6, 129.5, 129.1, 128.8, 128.1, 127.9, 127.0, 126.4, 125.9, 124.1, 66.7, 41.7, 41.5. ε_{366} = 2.4.

Phenacyl [N-(phenylacetyl)glycyl]glycinate (**1bPh**). White solid, yield 47%, m.p. 190–191 °C (ethanol). IR: 3244, 3084, 2928, 1750 (C=O); 1701 (C=O); 1687 (C=O); 1632 (C=O); 1535, 1451, 1283, 1223, 1197, 969, 755, 731, 689. ^{1}H NMR ($CDCl_3$): 7.99–7.96 m, 1 H, 7.89–7.87 m, 2 H, 7.66–7.58 m, 3 H, 7.51–7.46 m, 2 H, 7.26–7.17 m, 4 H (**Ph**$COCH_2$, **Ph**CH_2CON**H**-

CH_2CONH); 5.39 s, 2 H ($PhCOCH_2$); 4.06 d, 2 H, *J*($PhCH_2CONHCH_2CONHCH_2$,NH) = 5.6 ($PhCH_2CONHCH_2CONHCH_2$); 3.84 d, 2 H, *J*($PhCH_2CONHCH_2$,NH) = 5.6 ($PhCH_2CONHCH_2$); 3.53 s, 2 H ($PhCH_2CO$). ^{13}C NMR ($CDCl_3$): 190.4, 169.9, 168.4, 168.0, 134.2, 132.7, 131.2, 127.9, 127.6, 127.1, 126.4, 125.4, 65.2, 41.6, 41.4, 39.4. ε_{366} = 3.4.

Phenacyl [N-(1-naphthylacetyl)glycyl]glycinate (**1bNp**). White solid, yield 48%, m.p. 249–250 °C (ethanol/water 1:1). IR: 3327, 2928, 2851, 1751 (C=O); 1700 bs (2 × C=O); 1628 (C=O); 1536, 1438, 1312, 1245, 1199, 1088, 688, 654, 642. ^1H NMR ($CDCl_3$): 7.90–7.88 m, 1 H, 7.81–7.75 m, 4 H, 7.56–7.54 m, 1 H, 7.45–7.36 m, 6 H (**Ph**$COCH_2$, **Np**CH_2CO); 6.46 s, 1 H, 6.05 s, 1 H ($NpCH_2CONHCH_2CONH$); 5.29 s, 2 H ($PhCOCH_2$); 4.03 s, 2 H, 4.01 s, 2 H, 3.80 s, 2 H ($NpCH_2CONHCH_2CONHCH_2$). ^{13}C NMR ($CDCl_3$): 191.5, 171.9, 169.2, 134.4, 134.2, 134.1, 132.2, 130.8, 129.2, 128.9, 128.7, 128.0, 127.2, 126.5, 125.9, 123.7, 66.8, 43.4, 41.6, 41.2. ε_{366} = 3.9.

Phenacyl N-(phenylacetyl)valinate (**1cPh**). White solid, yield 52%, m.p. 114–115.0 °C (ethanol). IR: 3312, 3064, 2963, 1746 (C=O); 1698 (C=O); 1644 (C=O); 1537, 1189, 1154, 732, 686. ^1H NMR ($CDCl_3$): 7.90–7.87 m, 2 H, 7.63–7.59 m, 1 H, 7.51–7.46 m, 2 H, 7.38–7.26 m, 5 H (**Ph**$COCH_2$, **Ph**CH_2CO); 5.90 d, 1 H, *J*(NH,$PhCOCH_2OCOCH$) = 8.4; 5.48 d, 1 H, *J*(CH_2-A,CH_2-B) = 16.5 ($PhCOCH_2$-A); 5.22 d, 1 H, *J*(CH_2-A,CH_2-B) = 16.5 ($PhCOCH_2$-B); 4.71 dd, 1 H, *J*(NH,$PhCOCH_2OCOCH$) = 8.4 *J*($PhCOCH_2OCOCH$,$CH(CH_3)_2$) = 4.4 ($PhCOCH_2OCOCH$); 3.64 s, 2 H ($PhCH_2CO$); 2.35–2.25 m, 1 H ($CH(CH_3)_2$); 0.96 d, 3 H, *J*(CH,CH_3) = 6.9 ($CH(CH_3)_2$); 0.81 d, 3 H, *J*(CH,CH_3) = 6.9 ($CH(CH_3)_2$). ^{13}C NMR ($CDCl_3$): 191.7, 171.5, 170.1, 134.4, 134.2, 133.5, 129.6, 129.2, 129.1, 128.0, 66.6, 57.3, 44.0, 31.4, 19.3, 17.5. ε_{366} = 2.8.

Phenacyl N-(1-naphthylacetyl)valinate (**1cNp**). White solid, yield 51%, m.p. 117–118 °C (ethanol/water = 1:1). IR: 3278, 3060, 2963, 2928, 1745 (C=O); 1705 (C=O); 1655 (C=O); 1539, 1227, 1194, 963, 781, 687. ^1H NMR ($CDCl_3$): 7.94–7.91 m, 1 H, 7.80–7.73 m, 4 H, 7.55–7.37 m, 7 H (**Ph**$COCH_2$, **Np**CH_2CO); 5.71 d, 1 H, *J*(NH,$PhCOCH_2OCOCH$) = 8.9 (NH); 5.24 d, 1 H, *J*(CH_2-A,CH_2-B) = 16.5 ($PhCOCH_2$-A); 5.08 d, 1 H, *J*(CH_2-A,CH_2-B) = 16.5 ($PhCOCH_2$-B); 4.59 dd, 1 H *J*(NH,$PhCOCH_2OCOCH$) = 8.9, *J*($PhCOCH_2OCOCH$,$CH(CH_3)_2$) = 4.6 ($PhCOCH_2OCOCH$); 4.07 d, 1 H, *J*(CH_2-A,CH_2-B) = 16.5 ($NpCH_2CO$-A); 3.96 d, 1 H, *J*(CH_2-A,CH_2-B) = 16.5 ($NpCH_2CO$-B); 2.15–2.05 m, 1 H ($CH(CH_3)_2$); 0.72 d, 3 H, *J*(CH,CH_3) = 6.9 ($CH(CH_3)_2$); 0.57 d, 3 H, *J*(CH,CH_3) = 6.9 ($CH(CH_3)_2$). ^{13}C NMR ($CDCl_3$): 191.6, 171.3, 171.0, 134.2, 134.1, 131.2, 129.1, 129.0, 128.8, 128.5, 127.9, 126.3, 125.9, 124.1, 66.5, 57.1, 42.0, 31.2, 19.2, 17.2. ε_{366} = 3.1.

Phenacyl N-(phenylacetyl)phenylalaninate (**1dPh**). White solid, yield 56%, m.p. 179–180 °C (ethanol/water 4:1). IR: 3327, 3061, 3031, 2940, 1755 (C=O); 1699 (C=O); 1645 (C=O); 1529, 1449, 1217, 1169, 962, 728, 698. ^1H NMR ($CDCl_3$): 7.83–7.81 m, 2 H, 7.57–7.52 m, 1 H, 7.44–7.39 m, 2 H, 7.26–7.05 m, 8 H, 6.98–6.95 m, 2 H (**Ph**$COCH_2OCOCH(CH_2$**Ph**)-$NHCOCH_2$**Ph**); 5.75 d, 1 H, *J*(NH,$PhCOCH_2OCOCH$(CH_2Ph)NH) = 7.6 (NH); 5.38 d, 1 H, *J*(CH_2-A,CH_2-B) = 16.4 ($PhCOCH_2$-A); 5.20 d, 1 H, *J*(CH_2-A,CH_2-B) = 16.4 ($PhCOCH_2$-B); 4.91 m, 1 H ($PhCOCH_2OCOCH(CH_2Ph)NH$); 3.45 s, 2 H ($PhCH_2CO$); 3.21 dd, 1 H, *J*($PhCOCH_2OCOCH(CH_2Ph)NH$,CH_2Ph-A) = 5.6, *J*(CH_2-A,CH_2-B) = 14.0 (CH_2Ph-A); 3.02 dd, 1 H, *J*($PhCOCH_2OCOCH(CH_2Ph)NH$,CH_2Ph-B) = 7.0, *J*(CH_2-A,CH_2-B) = 14.0 ($PhCH_2$-B). ^{13}C NMR ($CDCl_3$): 195.0, 171.3, 171.2, 135.9, 134.8, 134.2, 129.5, 129.2, 128.8, 128.0, 127.5, 127.2, 66.7, 53.1, 43.8, 37.7. ε_{366} = 3.8.

Phenacyl N-(1-naphthylacetyl)phenylalaninate (**1dNp**). White solid, yield 50%, m.p. 197–198 °C (ethanol/water 1:1). IR: 3283, 3061, 3029, 2928, 1752 (C=O); 1701 (C=O); 1666 (C=O); 1542, 1229, 1185, 961, 782, 759, 707. ^1H NMR ($CDCl_3$): 7.91–7.80 m, 5 H, 7.64–7.59 m,

1 H, 7.53–7.46 m, 4 H, 7.43–7.36 m, 1 H, 7.32–7.30 m, 1 H, 7.11–6.97 m, 3 H, 6.75–6.73 m, 2 H (**Ph**COCH$_2$OCOCH(CH$_2$**Ph**)NHCOCH$_2$**Np**); 5.79 d, 1 H, *J*(PhCOCH$_2$OCOC**H**(CH$_2$Ph)N**H**) = 7.9 (NH); 5.37 d, 1 H, *J*(CH$_2$-A,CH$_2$-B) = 16.3 (PhCOC**H**$_2$-A); 5.23 d, 1 H, *J*(CH$_2$-A,CH$_2$-B) = 16.3 (PhCOC**H**$_2$-B); 4.98 m, 1 H (PhCOCH$_2$OCOC**H**(CH$_2$Ph)NH); 4.03 d, 1 H, *J*(CH$_2$-A, CH$_2$-B) = 16.3 (NpC**H**$_2$CO-A); 3.98 d, 1 H, *J*(CH$_2$-A,CH$_2$-B) = 16.3 (NpC**H**$_2$CO-B); 3.12 dd, 1 H, *J*(PhCOCH$_2$OCOC**H**(C**H**$_2$Ph)NH-A) = 5.5, *J*(CH$_2$-A,CH$_2$-B) = 14.0 (PhCOCH$_2$OCOCH-(C**H**$_2$Ph)NH-A); 2.97 dd, 1 H, *J*(PhCOCH$_2$OCOC**H**(C**H**$_2$Ph)NH-B) = 7.1, *J*(CH$_2$-A,CH$_2$-B) = 14.0 (PhCOCH$_2$OCOCH(C**H**$_2$Ph)NH-B). ^{13}C NMR (CDCl$_3$): 191.6, 171.1, 170.8, 135.8, 134.2, 134.1, 129.3, 129.1, 128.7, 128.5, 127.0, 126.3, 125.8, 124.0, 66.6, 53.0, 41.6, 37.6. ε_{366} = 4.2.

Phenacyl [N-(phenylacetyl)phenylalanyl]phenylalaninate (**1ePh**). White solid, yield 76%, m.p. 162–163 °C (ethanol). IR: 3296 bs, 3061, 3030, 2930, 1750 (C=O); 1708 (C=O); 1659 (C=O); 1642 (C=O); 1548, 1495, 1452, 1214, 1180, 974, 748, 698. ^{1}H NMR (CDCl$_3$): 7.94–7.91 m, 2 H, 7.68–7.63 m, 1 H, 7.55–7.50 m, 2 H, 7.31–7.21 m, 9 H, 7.10–7.03 m, 6 H (**Ph**COCH$_2$O-COCH(CH$_2$**Ph**)NHCH(CH$_2$**Ph**)NHCOCH$_2$**Ph**); 6.35 d, 1 H, *J*(NH,PhCOCH$_2$OCOC**H**) = 6.9 (PhCOCH$_2$OCOCH(CH$_2$Ph)N**H**); 5.81 d, 1 H, *J*(NH,C**H**NHCOCH$_2$Ph) = 7.3 (N**H**COCH$_2$Ph); 5.46 d, 1 H, *J*(CH$_2$-A,CH$_2$-B) = 16.3 (PhCOC**H**$_2$-A); 5.33 d, 1 H, *J*(CH$_2$-B,CH$_2$-A) = 16.3 (PhCOC**H**$_2$-B); 4.91 m, 1 H, 4.62 m, 1 H (PhCOCH$_2$OCOC**H**(CH$_2$Ph)NHC**H**); 3.54–3.43 m, 2 H (PhC**H**$_2$CO); 3.32 dd, 1 H, *J*(CH$_2$-A,PhCH$_2$CONHC**H**) = 5.1, *J*(CH$_2$-A,CH$_2$-B) = 14.1 (PhCH$_2$CONHCH(C**H**$_2$Ph)-A); 3.07 dd, 1 H, *J*(CH$_2$-B,PhCH$_2$CONHC**H**) = 7.6, *J*(CH$_2$-B,CH$_2$-A)= 14.1 (PhCH$_2$CONHCH(C**H**$_2$Ph)-B); 2.96 d, 2 H, *J*(PhCOCH$_2$OCOCH(C**H**$_2$Ph),PhCOCH$_2$O-COC**H**) = 6.6 (PhCOCH$_2$OCOCH(C**H**$_2$Ph)). ^{13}C NMR (CDCl$_3$): 191.6, 171.1, 170.8, 170.6, 136.4, 136.0, 134.4, 134.3, 129.6, 129.5, 129.3, 129.2, 128.8, 128.0, 127.7, 127.3, 127.1, 66.7, 54.2, 53.5, 43.8, 37.9, 37.5. ε_{366} = 4.2.

Phenacyl [N-(1-naphthylacetyl)phenylalanyl]phenylalaninate (**1eNp**). White solid, yield 36%, m.p. 181–182 °C (ethanol/water 4:1). IR: 3291 bs, 3062, 3032, 2928, 1752, 1700, 1648 bs, 1536, 1451, 1208, 1175, 967, 782, 753, 700. ^{1}H NMR (CDCl$_3$): 7.96–7.86 m, 5 H, 7.69–7.43 m, 6 H, 7.30–7.24 m, 4 H, 7.11–7.02 m, 5 H, 6.75–6.73 m, 2 H (**Ph**COCH$_2$OCOCH(CH$_2$**Ph**)-NHCH(CH$_2$**Ph**)NHCOCH$_2$**Np**); 6.28 d, 1 H, *J*(NH,NpCH$_2$CONHC**H**) = 7.3 (NpCH$_2$CON**H**); 5.68 d, 1 H, *J*(NH,PhCOCH$_2$OCOC**H**) = 7.9 (PhCOCH$_2$OCOCH(CH$_2$Ph)N**H**); 5.46 d, 1 H, *J*(CH$_2$-A,CH$_2$-B) = 16.3 (PhCOC**H**$_2$-A); 5.33 d, 1 H, *J*(CH$_2$-B,CH$_2$-A) = 16.3 (PhCOC**H**$_2$-B); 4.89 m, 1 H, 4.63 m, 1 H (PhCOCH$_2$OCOC**H**, NpCH$_2$CONHC**H**); 4.00 d, 1 H, *J*(CH$_2$-A,CH$_2$-B) = 16.5 (NpC**H**$_2$CO-A); 3.92 d, 1 H, *J*(CH$_2$-B,CH$_2$-A) = 16.5 (NpC**H**$_2$CO-B); 3.28 dd, 1 H, *J*(CH$_2$-A,NpCH$_2$CONHC**H**) = 5.3, *J*(CH$_2$-A,CH$_2$-B) = 14.1 (NpCH$_2$CONHCH(C**H**$_2$Ph)-A); 2.98 dd, 1 H, *J*(CH$_2$-B,NpCH$_2$CONHC**H**) = 7.8, *J*(CH$_2$-B,CH$_2$-A) = 14.1 (NpCH$_2$CONHCH-(C**H**$_2$Ph)-B); 2.81 d, 2 H, *J*(PhCOCH$_2$OCOCH(C**H**$_2$Ph),PhCOCH$_2$OCOC**H**) = 6.6 (PhCOCH$_2$O-COCH(C**H**$_2$Ph)). ^{13}C NMR (CDCl$_3$): 194.7, 171.1, 170.8, 170.5, 136.1, 134.5, 134.2, 132.2, 130.6, 129.5, 129.3, 129.2, 129.1, 128.8, 128.7, 128.6, 128.0, 127.3, 127.2, 127.0, 126.5, 125.9, 123.7, 66.7, 54.1, 53.5, 41.7, 37.9, 37.3. ε_{366} = 4.5.

Phenacyl N-methyl-N-(phenylacetyl)glycinate (**1fPh**). White solid, yield 46%, m.p. 93–94 °C (ethanol/water 1:1). IR: 3399, 3043, 2981, 2952, 1754 (C=O); 1698 (C=O); 1641 (C=O); 1438, 1415, 1370, 1179, 1112, 962, 795, 769, 701. ^{1}H NMR (CDCl$_3$): 7.92–7.90 m, 2 H, 7.65–7.60 m, 1 H, 7.53–7.48 m, 2 H, 7.32–7.24 m, 5 H (**Ph**COCH$_2$, **Ph**CH$_2$CO); 5.40 s, 2 H (PhCOC**H**$_2$); 4.36 s, 2 H (PhCOCH$_2$OCOC**H**$_2$); 3.81 s, 2 H (PhC**H**$_2$CO); 3.14 s, 3 H (NCH$_3$). ^{13}C NMR (CDCl$_3$): 191.9, 172.0, 169.0, 134.7, 134.2, 133.9, 129.1, 129.0, 128.8, 128.0, 127.0, 66.6, 49.6, 40.9, 37.2. ε_{366} = 2.4.

Phenacyl N-methyl-N-(1-naphthylacetyl)glycinate (**1fNp**). White solid, yield 23%, m.p. 103–104 °C (ethanol/water 1:1). IR: 3387, 3057, 2973, 2938, 1762 (C=O); 1701 (C=O); 1644

(C=O); 1449, 1407, 1376, 1183, 1116, 966, 790, 776, 690. ^{1}H NMR ($CDCl_3$): 7.97–7.86 m, 4 H, 7.78–7.77 m, 1 H, 7.66–7.61 m, 1 H, 7.56–7.41 m, 6 H (**Ph**$COCH_2$, **Np**CH_2CO); 5.42 s, 2 H (PhCOC**H**$_2$); 4.42 s, 2 H (PhCOCH_2OCOC**H**$_2$); 4.23 s, 2 H (NpC**H**$_2$CO); 3.21 s, 3 H (NCH_3). ^{13}C NMR ($CDCl_3$): 191.9, 172.2, 169.1, 134.3, 134.2, 132.2, 129.2, 129.0, 128.0, 126.8, 126.5, 125.9, 125.8, 123.7, 66.7, 49.7, 38.4, 37.3. ε_{366} = 2.9.

2-Oxo-2-(phenacyloxy)ethyl phenylacetate (**2Ph**). White crystals, yield 57%, m.p. 54–55 °C (methanol/water 8:2). For $C_{18}H_{16}O_5$ (312.3) calculated: 69.22% C, 5.16% H; found: 69.4% C, 2.47% H. IR: 3065, 2938, 1764 (C=O); 1731 (C=O); 1706 (C=O); 1425, 1392, 1207, 1154, 706. ^{1}H NMR ($CDCl_3$): 7.88–7.91 m, 2 H, 7.60–7.62 m, 1 H, 7.47–7.52 m, 2 H, 7.26–7.33 m, 5 H (all aromatic H); 5.40 s, 2 H (PhCOC**H**$_2$); 4.83 s, 2 H (PhCH_2COOC**H**$_2$); 3.76 s, 2 H (PhC**H**$_2$COO). ^{13}C NMR ($CDCl_3$): 191.3, 171.1, 167.5, 134.2, 133.6, 129.6, 129.1, 128.8, 128.0, 127.4, 66.7, 61.0, 40.9. EI MS, *m/z* (rel.%): 118 (40), 105 (100), 91 (56), 77 (23), 65 (10). ε_{366} = 1.7, ε_{313} = 65.9.

2-Oxo-2-(phenacyloxy)ethyl 1-naphthylacetate (**2Np**). White crystals, yield 63%, m.p. 83–84 °C (methanol/water 8:2). For $C_{22}H_{18}O_5$ (362.3) calculated: 72.92% C, 5.01% H; found: 73.92% C, 4.24% H. IR: 3067, 3008, 2946, 1770 (C=O); 1749 (C=O); 1699 (C=O); 1597, 1418, 1214, 1168, 1148, 781. ^{1}H NMR ($CDCl_3$): 8.00–8.04 m, 1 H, 7.79–7.89 m, 4 H, 7.59–7.64 m, 1 H, 7.40–7.562 m, 6 H (all aromatic H); 5.35 s, 2 H (PhCOC**H**$_2$); 4.82 s, 2 H (NpCH_2COOC**H**$_2$); 4.20 s, 2 H (PhC**H**$_2$COO). ^{13}C NMR ($CDCl_3$): 191.1, 170.9, 167.2, 134.0, 133.8, 132.1, 129.8, 128.9, 128.7, 128.2, 128.1, 127.7, 126.4, 125.8, 125.5, 123.8, 66.4, 60.9, 38.5. ε_{366} = 1.8, ε_{313} = 303.7.

Photokinetic Measurements

Quantum yield measurements: solutions of the bichromophores ($1–5 \times 10^{-3}$ mol l^{-1}) with triethylamine (0.001–0.5 mol l^{-1}) in acetonitrile were irradiated simultaneously at >366 nm, where only benzoyl group absorbs significantly[6], with 1-phenylbutan-1-one or 1-(4-methoxyphenyl)butan-1-one solutions used as actinometers in a "merry-go-round" apparatus immersed in a water bath. The samples were prepared by direct weighing the material into a volumetric flask or by dilution of stock solutions. Samples in Pyrex tubes were degassed in three freeze-pump-thaw cycles before sealing. The >366 nm bands from a medium-pressure 400 W Teslamp mercury lamp were isolated by filtration with Corning CS 0-52 and CS 7-37 filters. The photoproduct yields were analyzed by HPLC calibrated with authentic compounds. All quantum yields reported were calculated for photoproducts (acetophenone or 4-methoxyacetophenone) formation using methyl benzoate as the internal standard. The reaction conversions were kept under 15% to avoid the photoproduct interference.

All kinetic plots were linear with good correlation coefficients (≥0.95). This implies that triethylamine reacted only with one excited state of ketone. The consumption of the starting ketone and development of acetophenone was under detection limit in the absence of triethylamine even after 50 h of irradiation, which indicates that no other photochemical processes were involved. The laser flash photolysis experiments were carried out by exciting the sample solutions at 351 nm using a nanosecond excimer laser (XeF, ≈150 mJ pulses, 20 ns) in amino acid-based bichromophores[19].

Systematic PES Search and Molecular Dynamics Simulations

Conformational search was performed using the Single Coordinate Driving (SCD) methods implemented in the CICADA program[20]. All molecular mechanics calculations were per-

formed using the MM3 force field[21]. The following parameters were used for the conformational search: all conformations with a relative energy less than 20 kcal mol^{-1} were investigated; the single bonds of flexible linkage were systematically driven and peptide bonds were monitored only during the conformational search. The driven step was 25° for noncyclic torsions and 5° for torsions in a cycle. Only conformational pathways with barriers less than 90 kcal mol^{-1} were saved. All stationary points found on the potential energy hypersurface (PES) were then analyzed using the graph theory approach implemented in the program PANIC [22]. The geometry parameters of the retrieved conformations were monitored using the SCALP program[23].

Molecular dynamics (MD) simulations were carried out by the DYNAMIC program of the TINKER program package[24]. All MD simulations were performed at 300 K and a number of particles and pressure with the one-femtosecond integration step. All trajectories were 100 ns long and the coordinates of the system were saved every picosecond. The MM3 force field was used for the molecular mechanics calculations. The geometry parameters were monitored using the GOPENMOL program[25].

RESULTS

Photokinetic Measurements

The Hammond steady-state method[26] was applied to photokinetic ITET measurements in bichromophores investigated in this work. The electron transfer from triethylamine (TEA) and the following cleavage of a phenacyl ester[15] was chosen as a parallel process, which competes with the intramolecular triplet energy transfer between the chromophores. The measurements were based on comparison of the data for bichromophoric compounds (**1aNp**–**1fNp** and **2Np**) with those obtained for the model compounds (**1aPh**–**1fPh** and **2Ph**). While the exothermic energy transfer from the excited phenacyl chromophore ($T_1 \approx 73$ kcal mol^{-1}), with the unit intersystem crossing efficiency[27], to the naphthyl chromophore ($T_1 \approx 62$ kcal mol^{-1}) is highly efficient (Scheme 2a), no endothermic transfer is expected to the phenyl chromophore ($T_1 \approx 81$ kcal mol^{-1}) and the cleavage is the only process observed (Scheme 2b). The determination of the ITET efficiency is moreover standing on the assumption that naphthyl and phenyl derivatives of the same spacer should undergo the same reactions (such as nonradiative decay, hydrogen/electron abstraction, or bimolecular quenching) except that of ITET.

The quantum yield of acetophenone production Φ_R in the presence of an electron donor for bichromophores is expressed by Eq. (*1*):

$$\Phi_R = \phi_T \alpha \frac{k_R[\mathrm{TEA}]}{k_R[\mathrm{TEA}] + k_q[\mathrm{BC}] + k_d}, \qquad (1)$$

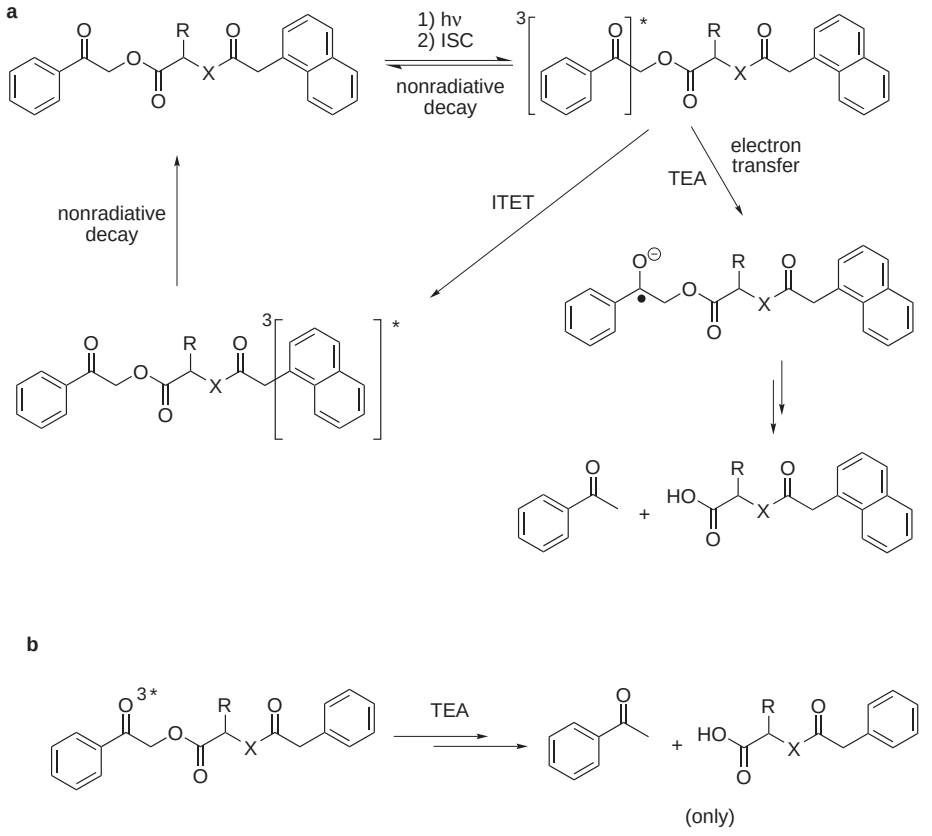

SCHEME 2

where ϕ_T is the quantum yield for the formation of triplet (the intersystem crossing quantum yield is unity in this case), α is the fraction of ketone radical-anion that does not undergo back electron transfer to amine cation, k_q is the rate constant for bimolecular quenching by naphthalene, [BC] is the concentration of the bichromophore, k_R is the rate constant of the electron transfer from TEA to the excited phenacyl, [TEA] is the concentration of triethylamine, and k_d is the overall rate constant for all inherent unimolecular deactivation pathways of the triplet excited state. Equation (*1*) can also be expressed for the model compounds with the absence of the k_q[BC] term.

Experimentally, a plot of Φ_R versus the electron donor concentration yields a curve which levels off to a limiting value $\Phi_R(\max)$ when $k_R[TEA] >> (k_q[BC] + k_d)$. The $\Phi_R(\max)$ value at the plateau is related to ϕ_T (= 1) and α by

$$\Phi_R(\max) \approx \phi_T \alpha \,. \tag{2}$$

Alternatively, a plot of $1/\Phi_R$ versus 1/[TEA], provides a straight line (Eq. (*3*)),

$$\frac{1}{\Phi_R} = \frac{1}{\phi_T \alpha}\left(1 + \frac{k_q[BC] + k_d}{k_R[TEA]}\right), \tag{3}$$

having intercept i with the y-axis ($i = 1/(\phi_T\alpha)$), and slope s for model compounds (Eq. (*4*))

$$s_{Ph} = \frac{k_d}{\phi_T \alpha k_R} \tag{4}$$

or bichromophores (Eq. (*5*))

$$s_{Np} = \frac{k_q[BC] + k_d}{\phi_T \alpha k_R} \,. \tag{5}$$

Provided that $\phi_T \alpha k_R^{Ph} = \phi_T \alpha k_R^{Ph}$, s^{Np}/s^{Ph} is related to the rates of unimolecular deactivation and reaction, which equals to

$$\frac{s_{Np}}{s_{Ph}} = \frac{k_q[BC] + k_d^{Np}}{k_d^{Ph}} \,. \tag{6}$$

The s^{Np}/s^{Ph} ratio reveals how many times is deactivation and bimolecular quenching of the naphthyl derivative faster than the deactivation of the phenyl model bichromophore. Thus, the higher is the value of the ratio s^{Np}/s^{Ph}, the faster ITET process is observed: the value is suitable for a comparison of the ITET rates in the studied bichromophores. To eliminate the contribution of bimolecular quenching in bichromophores, k_d^{Np}/k_d^{Ph} was calculated from Eqs (*4*) and (*5*) using the known values of $k_R = 2.2 \times 10^9$ l mol^{-1} s^{-1} [28], $k_q = 6 \times 10^9$ l mol^{-1} s^{-1} [29], and $\alpha = 0.70$ [30]. As a result, the k_d^{Np}/k_d^{Ph} ratios are the corresponding s^{Np}/s^{Ph} values corrected on the bimolecular quenching.

Table I presents the photokinetic data obtained in this work and clearly illustrates the differences in the ITET efficiencies in compounds that differ by the length of the interconnecting chain and its structure. Since the bimolecular quenching in bichromophores was found to be insignificant, the k_d^{Np}/k_d^{Ph} ratios are comparable to those of s^{Np}/s^{Ph}. While the k_d^{Np}/k_d^{Ph} ratios are high in **1c** (valine), **1f** (sarcosine) and **2** (diester), a relatively lower efficiency was found for **1a** (glycine; n = 1) **1b** (glycine; n = 2), **1d** (phenylalanine; n = 1), and **1e** (phenylalanine; n = 2). The tether length influence on the ratio is reflected in both the glycine and phenylalanine-based bichromophores. Two plots of $1/\Phi_R$ versus 1/[TEA] for **2** shown in Fig. 1 serve as an example.

NMR Analysis

Concentration dependences of the chemical shifts of NH group in **1aNp** were measured in order to identify possible intermolecular interactions (associations). An appropriate dilution technique[31] was used for determina-

TABLE I
Photokinetic parameters for bichromophores quenched by triethylamine[a]

Compound	s, mol l^{-1}	i	i/s, l mol^{-1}	Φ_R(max)	s^{Np}/s^{Ph}	k_d^{Np}/k_d^{Ph}
1aPh	0.0042	2.0	486	0.8	11.3	10.8
1aNp	0.0475	4.2	89	0.7		
1bPh	0.0260	2.7	102	0.5	5.2	5.2
1bNp	0.1358	4.5	33	0.3		
1cPh	0.0045	3.3	735	0.4	26.6	26.2
1cNp	0.1199	9.8	82	0.3		
1dPh	0.0177	3.8	215	0.4	7.0	7.0
1dNp	0.1246	6.2	50	0.3		
1ePh	0.0111	3.2	292	0.4	3.0	3.0
1eNp	0.0334	5.9	177	0.3		
1fPh	0.0194	1.0	50	0.9	35.3	35.3
1fNp	0.6849	1.4	2	0.8		
2Ph	0.0025	1.7	679	0.7	39.1	38.2
2Np	0.0977	9.2	94	0.5		

[a] The correlation coefficients of the linear dependences were >0.95.

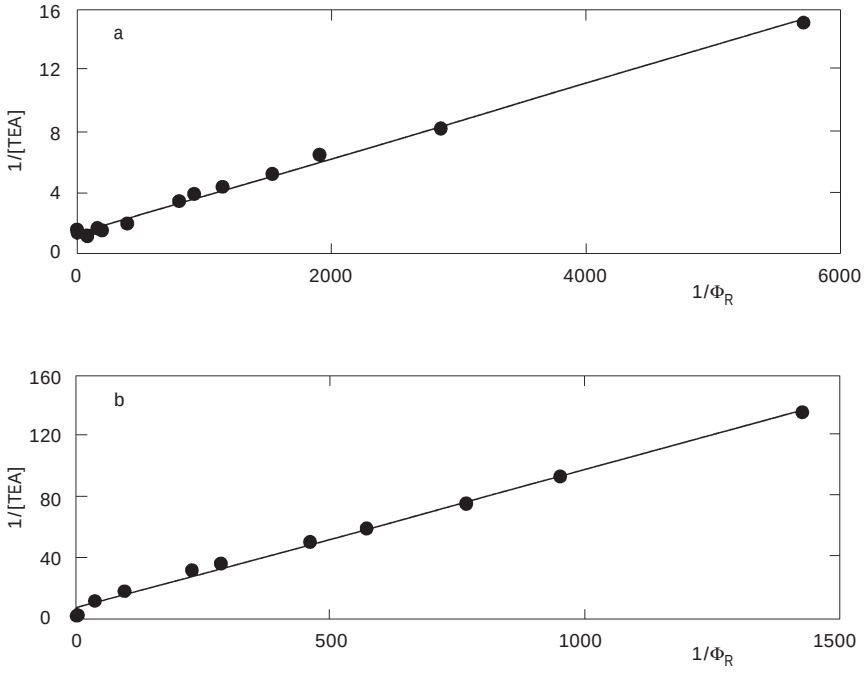

FIG. 1
The $1/\Phi_R$ versus 1/[TEA] dependences for **2Ph** (a) and **2Np** (b)

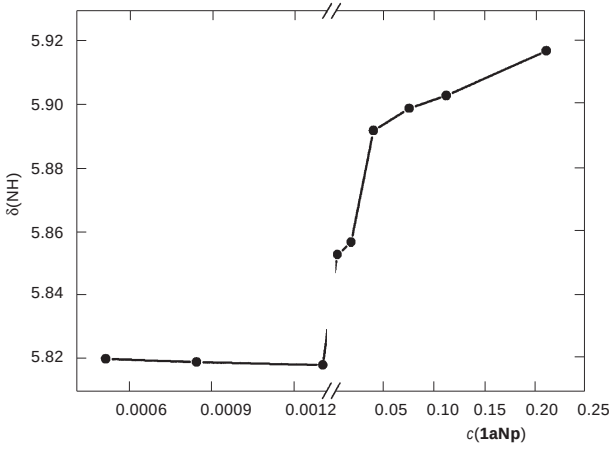

FIG. 2
Concentration dependence of chemical shift of NH resonance in **1aNp** (in $CDCl_3$)

tion of the concentration with minimal self-association. Figure 2 shows a sharp break in the concentration dependence of chemical shifts at concentration ≈2 × 10^{-3} mol l^{-1} where intermolecular association via hydrogen bonding becomes important.

In addition, NOESY NMR experiments were performed to investigate intramolecular hydrogen bond interactions in the corresponding bichromophores but, as expected, our experiments indicated that conformational changes of the studied bichromophores are too fast to be resolved by NMR.

X-ray Diffraction Analysis

We have recently reported the structures of diester **2Np** and corresponding amino acid **1aNp** determined by X-ray crystallographic analysis[32]. Both stretched structures revealed that the distance between the benzoyl and naphthyl chromophore is ≈9 Å in the solid state, which would not be sufficient for an efficient ITET by the electron-exchange mechanism. The intermolecular hydrogen bonds ≈1.98 Å in **1aNp** forming a hydrogen-bonded polymer were described.

Systematic PES Search and Molecular Dynamics Simulations

The calculated conformational populations having intentionally the center of the first (Np1) (a ring linked to the chain) or the second (Np2) ring of naphthalene in the average distance to the center of benzoyl aromatic ring (Ph) or benzoyl oxygen (O) (d_{PhNp1}, d_{PhNp2}, d_{ONp1}, d_{ONp2}) equal to or less than 4.2, 4.5 or 5.0 Å, are shown in Table II. The structures **1aNp** and **1bNp** (glycine) differ by the length of 3 atoms of the peptide moiety. While the O-Np2 contact dominates in **1aNp**, a longer bichromophore **1bNp** has the Np1 ring closer to the oxygen atom (O-Np1). The overlap of the π systems (Ph-Np) is then efficient only in **1bNp**. Compound **1cNp** (valine), providing a high k_d^{Np}/k_d^{Ph} value (Table I), gives a large conformational population even at very short fixed distances. On the other hand, the most efficient contact in **1dNp** (phenylalanine) is between Ph and Np1 but when the tether length increases by 3 atoms (**1eNp**), the interchromophoric distances considerably increase. Interestingly, the favorable populations in the sarcosine-based derivative (**1fNp**) in a comparison to **1aNp** are changed: while the O-Np2 contact dominates in **1aNp**, Ph-Np2 prevails in **1fNp**. The compound **2Np** (diester) has comparable populations for the Ph-Np contact as that of **1cNp**. Thus, our calculations show that the bichromophoric amino acids, dipeptides and diester are coiled in tighter conformations, which

determine the distances between chromophores well below 8 Å. The conformers with less than 3 or more than 8 Å interchromophore distances have a very low conformational population (<5%).

Molecular dynamics calculations were performed to obtain the frequencies of the coiling processes. The MD comparison of bichromophores **1aNp** and **2Np** gave quite similar results: an average time for the coiling was ≈200 or 70 ps to get aromatic rings (Ph-Np) or the oxygen atom and the naphthyl group (O-Np), respectively, to close proximity (4.5 Å). The simulations were run in vacuum where explicit molecules of solvent were not present. The influence of solvent molecules on the computational results presented here should be large and may reflect too fast coiling rates.

DISCUSSION

This work was inspired by our previous studies of the ITET rate constants in various flexible bichromophoric systems having a four-to-fifteen-atom interchromophore distance with polymethylene chain, D-$(CH_2)_x$-O-A, where D was benzoyl and A was naphthyl or biphenyl moiety[5,6]. The rate constants decreased only one order of magnitude as the number of atoms increased from 5 to 15. Furthermore, replacement of the polymethylene tether with polyoxyethylene oxide promoted better flexibility and so

TABLE II
The calculated populations χ of **1aNp**–**1fNp** and **2Np** (R^2 = 1-naphthyl) over all conformations having interchromophoric distances *d* less than a selected value

	χ, %											
	d_{PhNp1}			d_{PhNp2}			d_{ONp1}			d_{ONp2}		
	<4.2	<4.5	<5.0	<4.2	<4.5	<5.0	<4.2	<4.5	<5.0	<4.2	<4.5	<5.0
1aNp	0.0	0.0	0.4	0.0	0.0	11.3	8.8	8.8	8.9	0.9	73.9	74.3
1bNp	0.0	87.2	87.2	0.3	64.2	96.1	87.3	98.3	98.3	11.1	11.3	12.1
1cNp	25.6	47.9	68.7	10.1	12.3	54.1	37.5	40.0	51.3	61.7	69.4	69.6
1dNp	6.0	65.4	83.7	34.7	35.1	41.1	0.1	0.1	1.8	6.1	41.9	42.0
1eNp	0.0	1.3	12.7	2.6	9.7	13.0	73.3	73.4	77.1	12.0	13.4	15.1
1fNp	3.5	10.3	28.2	13.3	20.2	61.0	7.9	10.5	15.2	18.0	18.6	34.4
2Np	37.9	46.9	49.7	37.6	45.2	56.7	3.6	6.5	10.7	14.6	20.3	38.7

higher transfer rates. Here we examined shorter bichromophores having the general formula: D-link-A, where D is benzoyl, A is naphthyl, and the interconnecting chain (link) is an amino acid, dipeptide or diester tether (**1aNp**–**1fNp**, **2Np**). The tethers had 7 or 10 atoms, i.e. they were sufficiently long to allow coiling to a favorable conformation (F*), in which both chromophores are close enough for an efficient through-space energy transfer (k_{ET}) (Scheme 3; adapted according to[7]). It is well known that chromophores separated by 3–4 Å undergo instantaneous energy transfer and the conformational population with an interchromophore distance

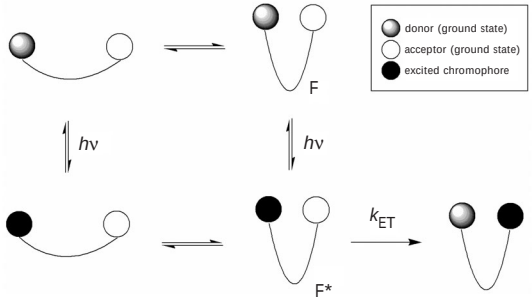

SCHEME 3

below 6 Å should contribute to the total transfer[11].

As was previously described[7,12], three distinct kinetic categories describe intramolecular energy transfer reactions: (i) ground-state control (k_{ET} is faster than the rate constants of conformational interconversions), (ii) conformational equilibrium (k_{ET} is slower than rates of conformational change), and (iii) rotation-controlled photochemical reaction (with comparable rate constants for both decay and irreversible conformational motion to a rapidly reacting conformer).

The bichromophoric molecules contained the donor benzoyl group that can transfer energy to the naphthyl acceptor or further react, providing two competing processes ("system clock"), of which the former is absent when naphthyl is replaced by phenyl (in model compounds). This allows to calculate the energy transfer efficiency as was utilized in some earlier energy transfer studies[5,6,33]. The competing reaction is based on the reactivity of phenacyl (benzoylmethyl) ester moiety which undergoes C–O bond scission in the presence of an electron-donating compound, presented by Falvey et al.[15,34], leading to the formation of acetophenone and the corresponding acid possibly via a triplet charge transfer complex[35,36].

The ITET rate constants in bichromophoric compounds could be expressed by Eq. (*7*),

$$k_{ET} = k_d^{Np} - k_d^{Ph} , \qquad (7)$$

where k_d is the overall rate constant of the corresponding unimolecular deactivation for 1-naphthyl (k_d^{Np}) and phenyl (k_d^{Ph}) derivatives. According to Eqs (3)–(5), the rate constants k_d can be calculated from *i*/*s* (Table I), equal to k_r/k_d or $k_r/(k_q[BC] + k_d)$ for model or bichromophoric compounds, respectively, and the known values of k_r and k_q (shown above). The calculated ITET rate constants k_{ET} were found in the order of 10^8 s^{-1} in the bichromophoric compounds of this study. This number, however, may serve only for a rough estimation and a check of the consistency of the kinetic measurements since the *i* values were biased by larger experimental errors. The result is in a good agreement with our preliminary results from laser flash photolysis[19] where k_{ET} were below the detection limit of the nanosecond laser (≈5 ns) and only measurements at low temperatures gave the rate constants of the order of 10^8 s^{-1}, close to the experimental values obtained with the polymethylene chromophores[6].

The main benefit of our photokinetic measurements is represented by the ratios s^{Np}/s^{Ph}, and consequently k_d^{Np}/k_d^{Ph} (Table I), serving for the evaluation of relative intramolecular triplet energy transfer rates in the studied bichromophores. Since the ratios are not affected by the values of $1/\Phi_R$ at the highest concentrations of the electron donor (as those of the *i* values), we have concluded that the k_d^{Np}/k_d^{Ph} ratios are more suitable for the ITET comparisons. It was assumed that the intermolecular hydrogen bonds in higher concentrations could affect the photokinetic data due to a more restricted molecular flexibility (intermolecular H-bonds) and bimolecular quenching. However, based on the NMR measurements (Fig. 1), none or minimal intermolecular self-association was observed in the study concentrations.

The value of k_d^{Np}/k_d^{Ph}, and so the relative ITET efficiency for the corresponding glycine-based bichromophore **1aNp** (seven-atom tether) was found to be higher for that of Gly-Gly derivative **1bNp** (ten-atom tether) by a factor of 2 (Table I). This indicates that the rate constants are somewhat sensitive to the number of interconnecting bonds as was observed, for example, in polymethylene bichromophores[6] or longer bichromophoric peptides[9]. The triplet-triplet energy transfer occurs by the electron-exchange mechanism which is expected to be allowed by a through-space mechanism

in all bichromophores studied. The through-bond transfer is known to be efficient only in shorter molecules with two-to-four interconnecting atoms[37], but the character of a partially conjugated peptide or ester chain could, nevertheless, contribute to the total energy transfer to a little extent. Comparable efficiencies indicate that the chain conformational motion must place the excited donor and ground state acceptor in a similar average interchromophore distances. The rigid planar peptide bond exists predominantly in trans conformation[38] and its partial double bond character (a rotation barrier of ≈20 kcal mol^{-1})[39] definitively causes substantial restrictions of the cis/trans free rotation. As a result, the amino acid-based short tether restricts only certain conformations and limits molecular dynamics. The estimated high rate constants $k_{ET} > 10^8$ s^{-1} (having the average interchromophore distance below 6 Å [7,40]) suggest that the observed bichromophore behavior might be described by the ground-state conformational distribution (an intramolecular equivalent of static quenching[41]). In such a model, a large portion of favorable geometries for an efficient energy transfer preexists already before excitation (in the ground state) and bond rotation to an unfavorable conformation would barely compete.

The computational conformational search provided a static picture of the conformational space and, thus, more or less thermodynamics-related information, while molecular dynamics showed the behavior of the system within a time scale[7]. The Boltzmann-weighted average distances afforded an information about the average distances in the steady-state conformational distribution, i.e., distribution of all realistically populated states at a given temperature. The differences in the chain length in **1aNp** and **1bNp**, for example, are reflected in variable favorable contacts between different parts of the chromophores (we have to realize that the excitation resides over the whole chromophore volume). The computations (Table II) nicely support comparable experimental ITET efficiencies found for those compounds. The more distant benzene ring of naphthyl (Np2) in **1aNp** is more available in the favorable geometries since the molecule is too short to allow Np1 to get closer to the benzoyl chromophore (visualized in Fig. 3). When the tether becomes longer (**1bNp**), Np1 is accessible at the expense of Np2.

In contrast, the ester-based bichromophore **2Np** underwent more efficient ITET than **1aNp** by a factor of 4. Flexibility of the diester chain is higher that that of the peptide system, which intuitively suggests a shift to the rotation-controlled photochemical reaction model. The stiffness of the peptide bond is greater than that of the ester bond because of the stronger double-bond character (C=N^+<) compared with (C=O^+–) resonance structure

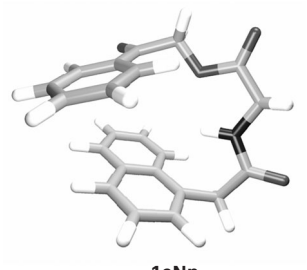

1aNp

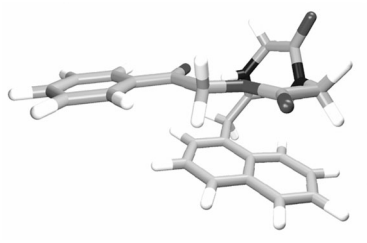

1bNp

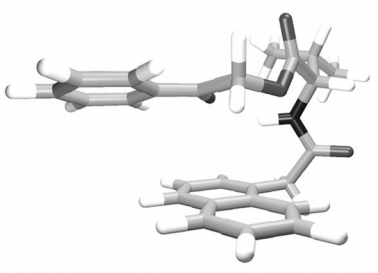

1cNp

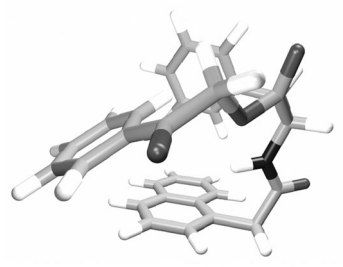

1dNp

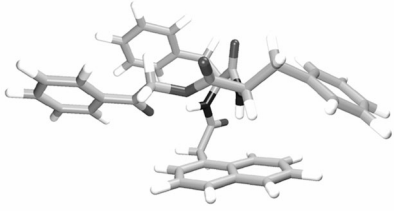

1eNp

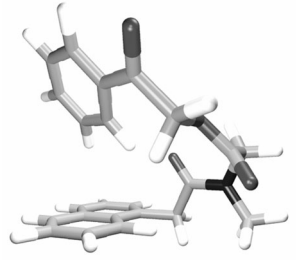

1fNp

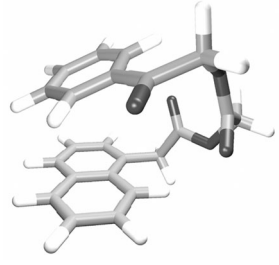

2Np

FIG. 3

The global energy minima of **1aNp**–**1fNp** and **2Np** (presented as the structures obtained by a systematic PES search)

(the energy barrier is <10 kcal mol^{-1})[42]. The calculated overlap populations in **2Np** (Table II) are evenly distributed for the π systems (Ph-Np) compared to **1aNp**, which may also advocate the higher efficiency in the former case. Alternatively, the X-ray diffraction analysis showed stretched structures of both compounds **1aNp** and **2Np** with the interchromophore distance of ≈9 Å in the solid state[32]. The replacement of the NH group by the oxygen atom did not cause any significant change of the structure. Such an information is, nevertheless, not very valuable for the studies in solution.

The photokinetic data also pointed out to an interesting effect of the chain side groups on the conformations of the studied bichromophores. The ITET efficiency increased in valine-based bichromophore **1cNp** over that of **1aNp**. Placing a relatively bulky isopropyl side group may reflect a less negative activation entropy in the contact conformations. The same effect is then attributed to an increase in the ITET efficiency in the sarcosine-based derivative (**1fNp**). Furthermore, the intramolecular H-bond in the glycine-based molecules is missing in **1fNp** due to the methyl substitution, which also significantly change the conformational behavior. In those molecules, preferred conformations situate both chromophores to a still closer proximity since one face of the molecule is hindered by the side chain as shown in Fig. 3.

Interesting enough was finding that the presence of a side group in **1cNp** and **1dNp** (they show a large difference in experimental ITET efficiencies) does not manifest itself so much in the population of favorable conformers but possibly by a preferred orientation of the chromophore moieties. One benzyl group in phenylalanine-based molecule **1dNp** or even two such groups in dipeptide **1eNp** suppressed the ITET efficiency. The computational simulation data did not provide a direct explanation for this behavior but a closer investigation revealed that the bulky benzyl group (**1dNp)** placed between both chromophores caused that their orientation was not parallel (to allow the most effective energy transfer due to an ideal π-orbital overlap[43]), as was observed in all other derivatives, but the aromatic rings were twisted by the angle of 30° (Fig. 3, **1dNp**; the phenacyl group is shown behind the benzyl group). The population of these twisted conformations is substantial and must indicate a decrease in the ITET efficiency but only in the case that fast rotation would not blur the energetically lower unfavorable orientation.

In conclusion, the application of the Hammond analysis[26] provided a tool capable of the intramolecular triplet energy efficiency measurements in (semi)flexible bichromophores. The work showed that the character as well as the length of the tether affects the efficiencies reflecting the system

flexibility and dynamics. A major conformational population (≈95%) has the interchromophore distances below 8 Å, which suggests that the ground-state model rather than the rotation control model describes best the photokinetic data obtained with the amino acid-based bichromophores.

We acknowledge the Ministry of Education, Youth and Sports of the Czech Republic for support of this research (MSM 143100005). We are indebted to Dr J. Wirz for stimulating discussion and the opportunity to use laser flash photolysis equipment. We thank to an anonymous reviewer for fruitful comments and suggestions.

REFERENCES

1. Dexter D. L.: *J. Chem. Phys.* **1953**, *21*, 836.
2. a) Turro N. J.: *Pure Appl. Chem.* **1977**, *49*, 405; b) Winnik M. A.: *Chem. Rev.* **1981**, *81*, 491.
3. Turro N. J.: *Modern Molecular Photochemistry*. Benjamin, Menlo Park (CA) 1978.
4. a) Cowan D. O., Baum A. A.: *J. Am. Chem. Soc.* **1971**, *93*, 1153; b) Katayama H., Maruyama S., Ito S., Tsujii Y., Tsuchida A., Yamamoto M.: *J. Phys. Chem.* **1991**, *95*, 3480; c) Lathioor E. C., Leigh W. J., St. Pierre M. J.: *J. Am. Chem. Soc.* **1999**, *121*, 11984, and references therein; d) Ito Y., Kawatsuki N., Giri B. P., Yoshida M., Matsuura T.: *J. Org. Chem.* **1985**, *50*, 2893; e) Wagner P. J., El-Taliawi G. M.: *J. Am. Chem. Soc.* **1992**, *114*, 8325.
5. Klán P., Wagner P. J.: *J. Am. Chem. Soc.* **1998**, *120*, 2198.
6. Wagner P. J., Klán P.: *J. Am. Chem. Soc.* **1999**, *121*, 9626.
7. Vrbka L., Klán P., Kříž Z., Koča J., Wagner P. J.: *J. Phys. Chem. A* **2003**, *107*, 3404.
8. McGimpsey W. G., Chen L., Carraway R., Samaniego W. N.: *J. Phys. Chem. A* **1999**, *103*, 6082.
9. Bieri O., Wirz J., Hellrung B., Schutkowski M., Drewello M., Kiefhaber T.: *Proc. Natl. Acad. Sci. U.S.A.* **1999**, *96*, 9597.
10. a) Lapidus L. J., Eaton W. A., Hofrichter J.: *Proc. Natl. Acad. Sci. U.S.A.* **2000**, *97*, 7220; b) Lapidus L. J., Eaton W. A., Hofrichter J.: *J. Mol. Biol.* **2002**, *319*, 19; c) Lapidus L. J., Steinbach P. J., Eaton W. A., Szabo A., Hofrichter J.: *J. Phys. Chem. B* **2002**, *106*, 11628.
11. Anderson R. W., Hochstrasser R. M., Lutz H., Scott G. W.: *J. Chem. Phys.* **1974**, *61*, 2500.
12. Wagner P. J.: *Acc. Chem. Res.* **1983**, *16*, 461.
13. Rather J. B., Reid E. E.: *J. Am. Chem. Soc.* **1919**, *41*, 75.
14. Newman M. S., Cella J. A.: *J. Org. Chem.* **1974**, *39*, 214.
15. Banerjee A., Falvey D. E.: *J. Org. Chem.* **1997**, *62*, 6245.
16. Narita M., Ogura T., Sato K., Honda S.: *Bull. Chem. Soc. Jpn.* **1986**, *59*, 2433.
17. Ringshaw D. J., Smith H. J.: *J. Chem. Soc.* **1964**, 1560.
18. Harada N., Ozaki K.: *Heterocycles* **1997**, *46*, 241.
19. Zabadal M., Wirz J., Klán P.: Unpublished results.
20. Koča J., Ludin M., Perez S., Imberty A.: *J. Mol. Graph. Model.* **2000**, *18*, 108.
21. a) Allinger N. L., Yuh Y. U., Lii J.-H.: *J. Am. Chem. Soc.* **1989**, *111*, 8551; b) Allinger N. L., Li F., Yan L.: *J. Comput. Chem.* **1990**, *11*, 848; c) Allinger N. L., Li F., Yan L., Tai J. C.: *J. Comput. Chem.* **1990**, *11*, 868; d) Lii J.-H., Allinger N. L.: *J. Am. Chem. Soc.* **1989**, *111*,

8566; e) Lii J.-H., Allinger N. L.: *J. Am. Chem. Soc.* **1989**, *111*, 8576; f) Lii J.-H., Allinger N. L.: *J. Phys. Org. Chem.* **1994**, *7*, 591; g) Lii J.-H., Allinger N. L.: *J. Comput. Chem.* **1998**, *19*, 1001.
22. Koča J.: *Prog. Biophys. Mol. Biol.* **1998**, *70*, 137.
23. Kříž Z.: *SCALP, Statit Conformational Analysis Program*. 1998 (unpublished).
24. Ponder J. W.: *TINKER – Software Tools for Molecular Design*. Washington University School of Medicine, St. Louis 1998.
25. a) Laaksonen L.: *J. Mol. Graphics* **1992**, *10*, 33; b) Bergman D. L., Laaksonen L., Laaksonen A.: *J. Mol. Graph. Model.* **1997**, *15*, 301.
26. a) Hammond G. S., Moore W. M.: *J. Am. Chem. Soc.* **1959**, *81*, 6334; b) Moore W. M., Hammond G. S., Foss R. P.: *J. Chem. Phys.* **1960**, *32*, 1594; c) Hammond G. S., Leermakers P. A.: *J. Am. Chem. Soc.* **1962**, *84*, 207.
27. Lamola A. A., Hammond G. S.: *J. Chem. Phys.* **1965**, *43*, 2129.
28. Bhattacharyya K., Das P. K.: *J. Phys. Chem.* **1986**, *90*, 3987.
29. Shizuka H., Yamaji M.: *Bull. Chem. Soc. Jpn.* **2000**, *73*, 267.
30. Cohen S. G., Stein N. M.: *J. Am. Chem. Soc.* **1971**, *93*, 6542.
31. a) Mizushima S., Shimanouchi T., Tsuboi M., Souda R.: *J. Am. Chem. Soc.* **1952**, *74*, 270; b) Yang D., Li B., Ng F.-F., Yan Y.-L., Qu J., Wu Y.-D.: *J. Org. Chem.* **2001**, *66*, 7303, and references therein.
32. Zabadal M., Heger D., Nečas M., Klán P.: *Acta Crystalogr., Sect. C: Cryst. Struct. Commun.* **2003**, *59*, 77.
33. a) Wagner P. J., Scheve B. J.: *J. Am. Chem. Soc.* **1979**, *101*, 378; b) Wagner P. J., El-Taliawi G. M.: *J. Am. Chem. Soc.* **1992**, *114*, 8325; c) Wagner P. J., Giri B. P., Frerking H. W., Jr., DeFrancesco J.: *J. Am. Chem. Soc.* **1992**, *114*, 8326.
34. a) Banerjee A., Lee K., Falvey D. E.: *Tetrahedron* **1999**, *55*, 12699; b) Banerjee A., Lee K., Yu Q., Fang A. G., Falvey D. E.: *Tetrahedron Lett.* **1998**, *39*, 4635.
35. Loutfy R. O., Loutfy R. O.: *Can. J. Chem.* **1972**, *50*, 4052.
36. Berger M., Camp R. N., Demetrescu I., Giering L., Steel C.: *Isr. J. Chem.* **1977**, *16*, 311.
37. a) Closs G. L., Piotrowiak P., Macinnis J. M., Fleming G. R.: *J. Am. Chem. Soc.* **1988**, *110*, 2652; b) Closs G. L., Johnson M. D., Miller J. R., Piotrowiak P.: *J. Am. Chem. Soc.* **1989**, *111*, 3751.
38. Song S., Asher S. A., Krimm S., Shaw K. D.: *J. Am. Chem. Soc.* **1991**, *113*, 1155.
39. Wiberg K. B., Laidig K. E.: *J. Am. Chem. Soc.* **1987**, *109*, 5935.
40. a) Terenin A., Ermolaev V. L.: *Trans. Faraday Soc.* **1956**, *52*, 1042; b) Ermolaev V. L.: *Sov. Phys. Dokl.* **1967**, *6*, 600.
41. Wagner P. J., Kochevar I.: *J. Am. Chem. Soc.* **1968**, *90*, 2232.
42. Wiberg K. B., Laidig K. E.: *J. Am. Chem. Soc.* **1987**, *109*, 5935.
43. a) Keller R. A.: *J. Am. Chem. Soc.* **1968**, *90*, 1940; b) Keller R. A., Dolby L. J.: *J. Am. Chem. Soc.* **1969**, *91*, 1293.